Check for updates

# Genomic Stability of Composite SCC*mec* ACME and COMER-Like Genetic Elements in *Staphylococcus epidermidis* Correlates With Rate of Excision

Nada Almebairik[1], Roxana Zamudio[1†], Corinne Ironside[2], Chaitanya Joshi[2], Joseph D. Ralph[1], Adam P. Roberts[3], Ian M. Gould[2], Julie A. Morrissey[1], Karolin Hijazi[2] and Marco R. Oggioni[1]*

[1] *Department of Genetics and Genome Biology, University of Leicester, Leicester, United Kingdom,* [2] *School of Medicine, Medical Sciences and Nutrition, University of Aberdeen, Aberdeen, United Kingdom,* [3] *Department of Tropical Disease Biology, Liverpool School of Tropical Medicine, Liverpool, United Kingdom*

The epidemiological success of methicillin-resistant *Staphylococcus aureus* USA300 has been associated with the presence of two mobile elements, the arginine catabolic mobile element (ACME) and the copper and mercury resistance (COMER) element. These two mobile elements are associated with resistance to copper, which has been related to host fitness and survival within macrophages. Several studies found that ACME is more prevalent, and exhibits greater diversity, in *Staphylococcus epidermidis* while COMER has not been identified in *S. epidermidis* or any other staphylococcal species. We aimed in this study to evaluate the presence and diversity of ACME and COMER-like elements in our *S. epidermidis* clinical isolates. The genomes of 58 *S. epidermidis* clinical isolates, collected between 2009 and 2018 in a Scottish hospital, were sequenced. A core-genome phylogenetic tree and genome based MLST typing showed that more than half of the isolates belong to the clinically predominant sequence type2 (ST2) and these isolates have been found to split into two lineages within the phylogenetic tree. Analysis showed the presence of SCC*mec* in the majority of isolates. Comparative analysis identified a cluster of ACME-positive isolates with most of them belonging to ST48. ACME showed high variation even between isolates of the same ACME type and ST. COMER-like elements have been identified in one of the two major hospital adapted drug resistant ST2 lineages; and showed high stability. This difference in stability at the genomic level correlates well with the up to one hundred times higher excision frequency found for the SCC*mec* elements in ACME-containing isolates compared to COMER-like element containing isolates. ACME/COMER-like element positive isolates did not show a significant phenotype of decreased copper susceptibility, while resistance to mercury was over-represented in COMER-like element

positive isolates. To the best of our knowledge, this is the first molecular characterization of COMER-like elements in *S. epidermidis* isolates. The presence of the COMER-like elements is the most prominent accessory genome feature of these successful lineages suggesting that this chromosomal island contributes to the success and wide clinical distribution of ST2 *S. epidermidis*.

## INTRODUCTION

*Staphylococcus epidermidis* and other coagulase negative staphylococci are a leading cause of nosocomial bloodstream and skin and soft tissue infections world-wide (Otto, 2009). Phylogenetic analyses have identified within the species *S. epidermidis* three major phylogenetic groups of hospital adapted isolates, two of ST2 and one of ST23 (Lee et al., 2018; Méric et al., 2018; Espadinha et al., 2019). The evolutionary pressure of the main nosocomial lineages is thought to be related to the hospital environment, but other evidence suggests that initial core genome changes in sequence type 2 (ST2) isolates result in increased acquisition of resistance traits (Lee et al., 2018). The important role of horizontal gene transfer in the evolution of *S. epidermidis* (Méric et al., 2018) and the well-established role of *Staphylococcus aureus* chromosomal cassette elements in bacterial fitness (Purves et al., 2018; Zapotoczna et al., 2018; Rosario-Cruz et al., 2019), suggest that the stepwise evolution of the cassette chromosomal elements and *mecA* gene is critical to spread of staphylococcal resistance, thus leading to the MRSA and MRSE epidemic (Rolo et al., 2017). The fine balance between acquisition and maintenance of accessory chromosomal elements shapes the evolutionary fitness of *S. epidermidis* (Zamudio et al., 2019).

The arginine catabolic mobile element (ACME) is a genomic island that first described in *Staphylococcus aureus* (MRSA) clone USA300 North American epidemic (USA300-NAE) and in *S. epidermidis* ATCC12228 (Diep et al., 2006; Planet et al., 2015). ACME is thought to increase the fitness of staphylococcus species by enhancing their ability to colonize skin and mucous membranes (Diep et al., 2008). ACME shows similar characteristics to the staphylococcal cassette chromosome *mec* (SCC*mec*) element in that it integrates into the staphylococcal chromosome at the attachment site *attB*, which is flanked by direct repeat sequences and is mobilized by the SCC*mec* encoded *ccrAB* genes. Moreover, ACME is known to commonly form a composite island with the SCC*mec* or SCC-associated genes (Diep et al., 2006; Planet et al., 2013; Lindgren et al., 2014; O'Connor et al., 2018a). To date, five distinct ACME types have been described in *S. epidermidis*; type I harbors the *arc* and *opp3* operons, type II harbors the *arc* operon only, type III harbors the *opp3* operon only, type IV harbors the *arc* and the *kdp* operons, and type V harbors all three *arc*, *opp3*, and *kdp* operons. The three characteristic gene clusters; *arc*, *opp3*, and *kdp* encode an arginine deaminase pathway, an oligopeptide permease ABC transporter and potassium ABC transporter respectively. Type IV and V ACME have been identified in oral *S. epidermidis* only (Diep et al., 2006; O'Connor et al., 2018a,b).

The copper and mercury resistance (COMER) mobile element was described for the first time in *S. aureus* (MRSA) strain USA300 South American epidemic (USA300-SAE) (Planet et al., 2015). This mobile element located in the USA300-SAE chromosome appears to replace ACME in USA300-NAE adjacent to the SCC*mec* type IV and it is thought to play a role in COMER which increases fitness as a result of increased survival to copper-mediated killing in macrophages (Planet et al., 2015; Purves et al., 2018; Zapotoczna et al., 2018). The COMER mobile element is associated with an abortive phage infection system and two main gene clusters, the *mer* operon composed of the *merR/A/B* genes and the *cop* operon composed of the *copB/L/mco* genes (Planet et al., 2015; Purves et al., 2018). To date, the COMER mobile element has not been detected in *S. epidermidis* strains.

This study investigated the prevalence and evolution of ACME and COMER mobile elements in 58 *S. epidermidis* clinical isolates retrieved from blood samples. ACME and COMER were detected and characterized using whole genome sequencing (WGS) analysis. This analysis revealed the presence of several variations of ACME as well as detection of previously undescribed COMER-like element in 11 *S. epidermidis* isolates. The excision and circularization of the ACME and COMER-like elements was investigated.

## MATERIALS AND METHODS

### Bacterial Isolates

A collection of 58 *S. epidermidis* clinical isolates collected between 2009 and 2018 from blood cultures of patients admitted to the ICU of Aberdeen Royal Infirmary (Aberdeen, United Kingdom) were investigated in this study (**Table 1**). Twenty-five of these isolates were analyzed previously for their biocide resistance gene content (Hijazi et al., 2016). The *S. epidermidis* strains were stored at −80°C in tryptic soy broth (TSB, BD, France) with 50% glycerol (Thermo Fisher Scientific, United Kingdom). The strains were streaked on tryptic soy agar (TSA) plates (prepared by adding 1.5% agarose to TSB) and incubated at 37°C for 16–24 h. Single colonies were then sub-cultured in TSB and incubated overnight at 37°C/200 rpm in a shaking incubator (Innova 4000, New Brunswick Scientific, United Kingdom).

### Whole Genome Sequencing

Genomic DNA extraction was performed using NucleoSpin Tissue Kit (Macherey-Nagel, Germany) following the manufacturer's instructions. Genomic DNA was eluted in 30 µl pure water, and the concentration and purity measured

**TABLE 1 |** *S. epidermidis* isolates.

| | Isolate | Accession | Date | MLST | COMER-like | ACME | SCC*mec* type |
|---|---|---|---|---|---|---|---|
| NB22338Q | STAPH 48 | SAMN12840226 | July 2009 | ST559 | | | SCC*mec*-IV |
| NB23267V | STAPH 49 | SAMN12840227 | July 2009 | ST2 | COMER | | SCC*mec*-III |
| NB41003Z | STAPH 51 | SAMN12840228 | May 2010 | ST83 | | | SCC*mec*-IV |
| NB14428Z | STAPH 53 | SAMN12840229 | May 2010 | ST5 | | ACME-V | SCC*mec*-IV |
| NB21991B | STAPH 54 | SAMN12840230 | July 2010 | ST5 | | | SCC*mec*-IV |
| NB24551C | STAPH 56 | SAMN12840231 | August 2010 | ST2 | | | SCC*mec*-IV |
| NB06465P | STAPH 58 | SAMN12840232 | March 2011 | ST2 | | | SCC*mec*-IV |
| NB12208Q | STAPH 59 | SAMN12840233 | April 2011 | ST83 | | | SCC*mec*-IV |
| NB24506S | STAPH 60 | SAMN12840234 | August 2011 | ST2 | COMER | | SCC*mec*-III |
| NB25777X | STAPH 61 | SAMN12840235 | September 2011 | ST2 | COMER | | SCC*mec*-III |
| NB26250A | STAPH 62 | SAMN12840236 | September 2011 | ST2 | COMER | | SCC*mec*-III |
| NB26865Y | STAPH 63 | SAMN12840237 | September 2011 | ST2 | COMER | | SCC*mec*-III |
| NB28476A | STAPH 64 | SAMN12840238 | October 2011 | ST2 | COMER | | SCC*mec*-III |
| NB13883R | STAPH 66 | SAMN12840239 | April 2012 | ST19 | | | |
| NB25117Z | STAPH 67 | SAMN12840240 | July 2012 | ST210 | | | |
| NB25100R | STAPH 68 | SAMN12840241 | July 2012 | ST54 | | ACME-I | |
| NB29474S | STAPH 69 | SAMN12840242 | September 2012 | ST2 | | | SCC*mec*-IV |
| NB41238E | STAPH 70 | SAMN12840243 | December 2012 | ST2 | | | SCC*mec*-IV |
| NB01101D | STAPH 73 | SAMN12840244 | January 2013 | ST204 | | | |
| NB02243Y | STAPH 74 | SAMN12840245 | January 2013 | ST470 | | ACME-IV | |
| NB03947K | STAPH 75 | SAMN12840246 | January 2013 | ST2 | COMER | | SCC*mec*-III |
| NB22235H | STAPH 77 | SAMN12840247 | January 2013 | ST59 | | | SCC*mec*-IV |
| NB26073F | STAPH 78 | SAMN12840248 | July 2013 | ST2 | COMER | | SCC*mec*-III |
| NB33101Z | STAPH 79 | SAMN12840249 | September 2013 | ST48 | | ACME-I | SCC*mec*-IV |
| NB671022 | STAPH 83 | SAMN12840250 | February 2014 | ST2 | | | SCC*mec*-IV |
| NB03169X | STAPH 1 | SAMN12840193 | January 2016 | ST2 | COMER | | SCC*mec*-III |
| NB03186T | STAPH 2 | SAMN12840194 | January 2016 | ST35 | | ACME-I | SCC*mec*-IV |
| NB09909V | STAPH 3 | SAMN12840195 | March 2016 | ST48 | | ACME-I | SCC*mec*-IV |
| NB10503A_1 | STAPH 4 | SAMN12840196 | March 2016 | ST59 | | | SCC*mec*-IV |
| NB10503A_2 | STAPH 5 | SAMN12840197 | March 2016 | ST5 | | | SCC*mec*-IV |
| NB11089T | STAPH 6 | SAMN12840198 | March 2016 | ST5 | | | SCC*mec*-IV |
| NB11582T | STAPH 7 | SAMN12840199 | April 2016 | ST2 | | | SCC*mec*-IV |
| NB12943Y | STAPH 8 | SAMN12840200 | April 2016 | ST2 | COMER | | SCC*mec*-III |
| NB13468Z | STAPH 9 | SAMN12840201 | April 2016 | ST23 | | | SCC*mec*-IX |
| NB13483J | STAPH 10 | SAMN12840202 | April 2016 | ST2 | COMER | | SCC*mec*-III |
| NB17762B | STAPH 12 | SAMN12840203 | May 2016 | ST528 | | ACME-I | |
| NB18619Q | STAPH 13 | SAMN12840204 | June 2016 | ST2 | | | SCC*mec*-IV |
| NB20483A | STAPH 14 | SAMN12840205 | June 2016 | ST2 | | | SCC*mec*-IV |
| NB21362A | STAPH 15 | SAMN12840206 | June 2016 | ST2 | | | SCC*mec*-IV |
| NB24986M | STAPH 16 | SAMN12840207 | July 2017 | ST54 | | ACME-I | SCC*mec*-IV |
| NB24987J | STAPH 17 | SAMN12840208 | July 2017 | ST210 | | ACME-IV | SCC*mec*-IV |
| NB31156H | STAPH 18 | SAMN12840209 | September 2017 | ST65 | | | |
| NB31437E | STAPH 19 | SAMN12840210 | September 2017 | ST73 | | ACME-II | |
| NB34495N | STAPH 20 | SAMN12840211 | October 2017 | ST2 | | | SCC*mec*-IV |
| NB36056Y | STAPH 21 | SAMN12840212 | October 2017 | ST2 | | | SCC*mec*-IV |
| NB36246W | STAPH 22 | SAMN12840213 | October 2017 | ST210 | | ACME-IV | SCC*mec*-V |
| NB37325D | STAPH 23 | SAMN12840214 | October 2017 | ST2 | | | SCC*mec*-IV |
| NB37754V_1 | STAPH 24 | SAMN12840215 | October 2017 | ST2 | | | SCC*mec*-IV |
| NB37754V_2 | STAPH 25 | SAMN12840216 | October 2017 | ST591 | | | SCC*mec*-IV |
| NB38801E | STAPH 27 | SAMN12840217 | November 2017 | ST2 | | | SCC*mec*-IV |
| NB40693L | STAPH 28 | SAMN12840218 | November 2017 | ST2 | | | SCC*mec*-IV |
| NB41771A | STAPH 29 | SAMN12840219 | November 2017 | ST2 | | | SCC*mec*-IV |

*(Continued)*

TABLE 1 | Continued

|         | Isolate  | Accession    | Date          | MLST | COMER-like | ACME   | SCC*mec* type |
|---------|----------|--------------|---------------|------|------------|--------|---------------|
| NB42838N | STAPH 30 | SAMN12840220 | December 2017 | ST2  |            |        | SCC*mec*-V    |
| NB43408J | STAPH 31 | SAMN12840221 | December 2017 | ST2  |            |        | SCC*mec*-V    |
| NB03117S | STAPH 32 | SAMN12840222 | January 2018  | ST2  |            |        | SCC*mec*-IV   |
| NB03149G | STAPH 33 | SAMN12840223 | January 2018  | ST2  |            |        | SCC*mec*-IV   |
| NB05012Y | STAPH 34 | SAMN12840224 | January 2018  | ST48 |            | ACME-I | SCC*mec*-IV   |
| NB05684Z | STAPH 35 | SAMN12840225 | February 2018 | ST48 |            | ACME-I | SCC*mec*-IV   |

by the NanoDrop 2000c spectrophotometer (Thermo Fisher Scientific, United Kingdom). Genomic DNA was sequenced on a HiSeq 4000 sequencer (Illumina, The Wellcome Trust Centre for Human Genetics at the University of Oxford) with 150 bp paired-end reads. Genome sequences were trimmed using Trimmomatic (Bolger et al., 2014), then assembled using SPAdes software version v3.9.0 (Nurk et al., 2013) and quality-assessed with QUAST (Gurevich et al., 2013). The draft genomes in contig level for all 58 isolates were submitted to the GenBank under the project number PRJNA574294, the GenBank accession number for the isolates is shown in **Table 1**.

## Multilocus Sequence Typing (MLST) and Core-Genome Phylogeny Tree

The sequence type (ST) of each isolate was specified by submitting the whole genome sequence (WGS) to the *S. epidermidis* MLST 2.0 online database (Larsen et al., 2012). The core-genome alignment was generated using Roary software version 3.11.2 (Page et al., 2015). Then a maximum likelihood tree for 58 Aberdeen isolates and the BPH0662 reference genome was build using RAxML software version 8.2.X (Stamatakis, 2014). Rstudio v 1.1.453[1] and the R package ggtree v 1.13.5 (Yu et al., 2017) was used for visualization and annotation of the phylogeny tree.

Maximum likelihood tree for the 58 Aberdeen isolates and 225 isolates from Lee's collection (NCBI BioProject numbers: PRJEB12090, PRJNA470534, and PRJNA470752) (Lee et al., 2018) and the BPH0662 reference genome (doi: 10.1099/mgen.0.000077) was generated through the iqtree tool (doi: 10.1093/molbev/msu300) by using the Hasegawa–Kishino–Yano model and gamma distribution (Yang, 1994) (doi: 10.1007/bf00160154).

## Identification of SCC*mec*, ACME, and COMER-Like Elements

For each isolate, the presence and the type of the SCC*mec* mobile element was determined by submitting the genome sequence to the SCC*mec*Finder 1.2 online database (Kaya et al., 2018). Contigs were aligned to the ACME and COMER elements previously characterized in *S. aureus* USA300 strain FPR3757 (GenBank accession number CP000255) and strain CA12 (GenBank accession number CP007672) respectively using the BLAST software (AltschuP et al., 1990) in order to detect the presence of ACME and COMER elements in the study isolates. In

some isolates the ACME and COMER element-associated genes were identified on three and five separate contigs – in this case ACME-I and COMER elements were assembled by PCR. These contigs were organized, reoriented and assembled using BLAST software, Reverse complement tool[2] and ISfinder online database (Siguier, 2006). For further investigations, contigs were annotated using the RAST server (Aziz et al., 2008), Artemis sequence viewer (Berriman, 2003) and SnapGene viewer (GSL Biotech)[3]. This is followed by multiple alignment of the ACME and COMER mobile elements using Mauve software to detect the variation in these elements among the isolates (Darling, 2004).

## Metal Susceptibility

The susceptibility of these isolates to several metals including copper sulfate ($CuSO_4$), nickel sulfate ($NiSO_4$), iron chloride ($FeCl_3$), manganese sulfate ($MnSO_4$), zinc sulfate ($ZnSO_4$), cobalt bromide ($CoBr_2$), cadmium chloride ($CdCL_2$), mercuric chloride ($HgCl_2$), and sodium arsenate ($AsNA_2$) (all Sigma) was determined using disc diffusion testing. Several colonies from overnight TSA cultures were collected with a sterile loop and re-suspended into Mueller Hinton broth (Oxoid, United Kingdom) to $OD_{600}$ = 0.5. A Mueller Hinton agar (MHA) plate was seeded with the culture using a sterile swab in three different directions to obtain uniform growth. Ten microliter of 1M solutions of each metal were loaded into a sterile filter discs, obtained from filter papers (Munktell, United Kingdom), and allowed to dry for 15 min. Filter discs were then firmly applied to the surface of the MHA plate and incubated overnight at 37°C. The metal susceptibility was determined using the epidemiological cut-off values (ECOFF) (Morrissey et al., 2014) followed by Fisher's Exact test to find the susceptibility association among the isolates[4]. A linear regression model was applied to predict the disk diffusion values based on the presence or absence of the composite element by using the lm function from stats's R package.

## Site-Specific Excision of SCC*mec*, ACME, and COMER-Like Elements

A qPCR-based method was used to quantify the rate of excision and circularization of the composite SCC*mec* and ACME/COMER-like elements. Specific primers were designed using SnapGene viewer software (**Table 2**) and used to amplify

---

[1]www.rstudio.com/

[2]www.bioinformatics.org/sms/rev_comp.html

[3]Snapgene.com

[4]https://www.socscistatistics.com

| Primers | Sequence | Annealing temperature (°C) |
|---------|----------|---------------------------|
| **SCC*mec*-IV AND ACME PRIMERS** | | |
| qAttR1 fw | TACGCTCTATCATTCAGCACTATGA | 55 |
| qAttR1 rev | ATGATAAGCTTCTTAAAAACATAACAGC | 55 |
| Probe R1 | CACCAAATGATGCGCGTCATATTGATAGA | 61 |
| qAttR2 fw | AAACCAAAGTCGATATCATCATTTTG | 55 |
| qAttR2 rev | CAGCATTATCGTAAGTTAACTACATT | 55 |
| Probe R2 | CGACTTTAATTATAAAAAACCGCACTCTTAACCG | 61 |
| qAttL fw | GAAGTGATTTTACGATATCACCTTCT | 55 |
| qAttL rev | CATTTAAGATGGAATTCAAATTTTATTTTACTTTC | 54 |
| Probe L | TATATTTCAGTAGGCACCGACGTATACAGAATCA | 61 |
| **SCC*mec*-III AND COMER-LIKE PRIMERS** | | |
| qAttR1 fw | CTCTCTTAAATTTTTGTTTGATTAGATTAGACC | 56 |
| qAttR1 rev | ACTTGAAATGAAAGACTGCGG | 56 |
| Probe R1 | ACGCATTCAATATGTCTACACGTGAATTTAGTCT | 62 |
| qAttR2 fw | ACACCAGCTTTCTATGTAGGTAA | 55 |
| qAttR2 rev | ATTTTATTGGAGATACTATATACTTAACCAATTTC | 54 |
| Probe R2 | GCGAAGAAAGCCATTATTATGAGGTGATTGTAG | 61 |
| qAttL fw | GAGCGACAAATTCCAATGTAATAGTA | 55 |
| qAttL rev | ACCAAACAATGAATATATAATACATTTAAGATG | 54 |
| Probe L | GTCGCTCTTTCGTTTCAGTTAAGGAAAATG | 61 |

the element attachment sites, the circularized SCC*mec* and SCC*mec* plus the ACME/COMER-like element and the excision products (chromosome junction after the element excision). Excision of the SCC*mec* and ACME/COMER-like element was induced in selected isolates using 0.5 µg/ml Mitomycin C (Sigma-Aldrich). qPCR reactions were performed using the TaqMan Fast Advanced Master Mix (Thermo Fisher Scientific) with the following run protocol: initial denaturation step at 95°C for 20 s then 45 cycles of 95°C for 3 s and 60°C for 30 s. The reactions were carried out in MiroAmp Fast 96-Well Reaction Plate (Applied biosystems) using a 7500 real-time PCR machine (Applied Biosystems). The rate of excision was measured using qPCR by comparing the excised circularized element and the reconstituted chromosomal attachment site to the integrated element using this formula: $2^{-\Delta CT}$ (Livak and Schmittgen, 2001).
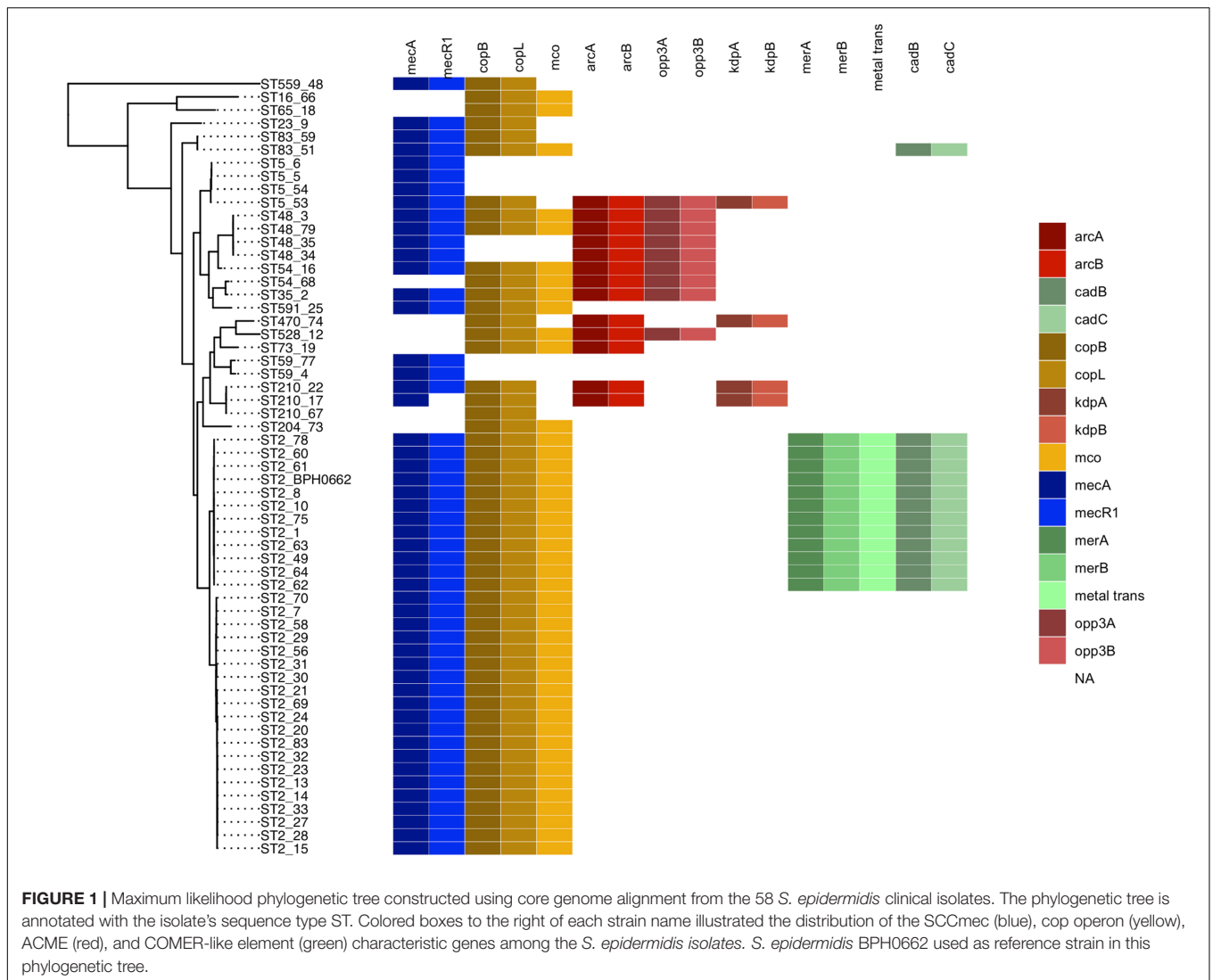
## RESULTS

The evolution of *S. epidermidis* isolates recovered from bloodstream infections between 2009 and 2018 at Aberdeen Royal Infirmary was studied by core-genome phylogenetic analysis (**Figure 1**). Genome-based MLST revealed that more than 50% of the isolates (31 of 58) belong to the major hospital acquired multidrug resistant ST2 lineage which in turn was found to separate into two sub-lineages as previously described (Lee et al., 2018). The other 16 STs were distributed among different lineages in the phylogenetic tree. Four ST5 isolates, four ST48 isolates and three ST210 isolates. Of the 58 *S. epidermidis* isolates, 86% (50/58) were methicillin resistant *S. epidermidis* (MRSE) as

they harbored the *mecA* gene. The vast majority of these MRSE contained SCC*mec* types III and IV (**Table 1**). The other eight isolates (14%) considered methicillin sensitive *S. epidermidis* (MSSE) lacked the *mecA* gene. All the isolates harbored the penicillin resistance *blaZ* gene except isolate STAPH74.

Eleven of the 31 isolates belonging to the clinically predominant ST2 (35%) were found to be positive for a COMER-like element (**Figure 1**). These eleven isolates were clustered in one of the two ST2 sub-lineages, also containing the reference isolate BPH0662 (doi: 10.1099/mgen.0.000077) (Lee et al., 2018). We have named this element COMER-like element as it harbored the *mer* and *cop* operons as well as *abi* gene that exhibited very high nucleotide sequence identity with the *mer/cop* operons (99.98% identity over 11,028 bp) and *abi* gene cluster (100% identity over 1,197 bp) located on the COMER element of MRSA USA300 strain CA12 (GenBank accession number CP007672) (**Figure 2**). However, additional genes not present in COMER USA300, including *ars* operon and a type I restriction modification system, were identified in the *S. epidermidis* COMER-like elements. The COMER-like element was found to be a composite island of 99.2 kb in size. The structural organization of this composite island was identical in all eleven isolates with the COMER-like element located immediately downstream of SCC*mec*-III and encoding the *mecA* gene and the *cad/mer* operons with > 99.8% nucleotide sequence identity with the corresponding genes in SCC*mec*-III of strain 85/2082 (GenBank accession number AB037671). Additionally, this composite island contained a module harboring the *speG* and *ccrAB4* genes and the gene of a putative further metal transporter (locus_tag = ''F9B38_12675) (**Figure 2**). In contrast to our composite *S. epidermidis* element, the COMER element in USA300 is located downstream of SCC*mec*-IV (**Figure 2**). This is the first description of a COMER-like element in *S. epidermidis* strains.

The arginine catabolic mobile element (ACME) was detected in 9/50 (18%) of the MRSE isolates and 4/8 of the MSSE isolates (**Figure 1**). These ACMEs encoded the *arc* and/or *opp3* and/or *kdp* operons as previously described for ACME in *S. epidermidis* (Miragaia et al., 2009; Barbier et al., 2011; Onishi et al., 2013; Soroush et al., 2016; McManus et al., 2017; O'Connor et al., 2018a). The ACME-I element was the predominant ACME type and all ACME-I containing isolates, except isolate STAPH12 (ST528), found to cluster in one lineage in the phylogenetic tree containing ST48, ST54 and ST35. The ACME-I element in these isolates was assembled and found to harbor the *arc, opp3* operons, and the *speG* gene, all flanked by 15 bp direct repeats (DR_B and DR_C). Additionally, one or more modules were found to colocalize with the ACME-I forming a composite island (**Figure 3**). Comparative analysis tools showed high variability of ACME-I composite island. In 3 out 7 isolates [ST48 (*n* = 2) and ST54 (*n* = 1)], the ACME-I was located downstream of the SCC*mec*-IV, separated by a module composed of *ars* and *cop* genes. This module and the SCC*mec*-IV were flanked by DR_A and B respectively at the 5'end in *orfX* (**Figure 3A**). In 2 out 7 ST48 isolates the ACME-I element colocalized with SCC*mec*-IV but lacked the *ars/cop* gene modules (**Figure 3B**). In one ST35 isolate an additional module harboring the *ccrAB4* genes flanked

**FIGURE 1 |** Maximum likelihood phylogenetic tree constructed using core genome alignment from the 58 *S. epidermidis* clinical isolates. The phylogenetic tree is annotated with the isolate's sequence type ST. Colored boxes to the right of each strain name illustrated the distribution of the SCCmec (blue), cop operon (yellow), ACME (red), and COMER-like element (green) characteristic genes among the *S. epidermidis isolates. S. epidermidis* BPH0662 used as reference strain in this phylogenetic tree.
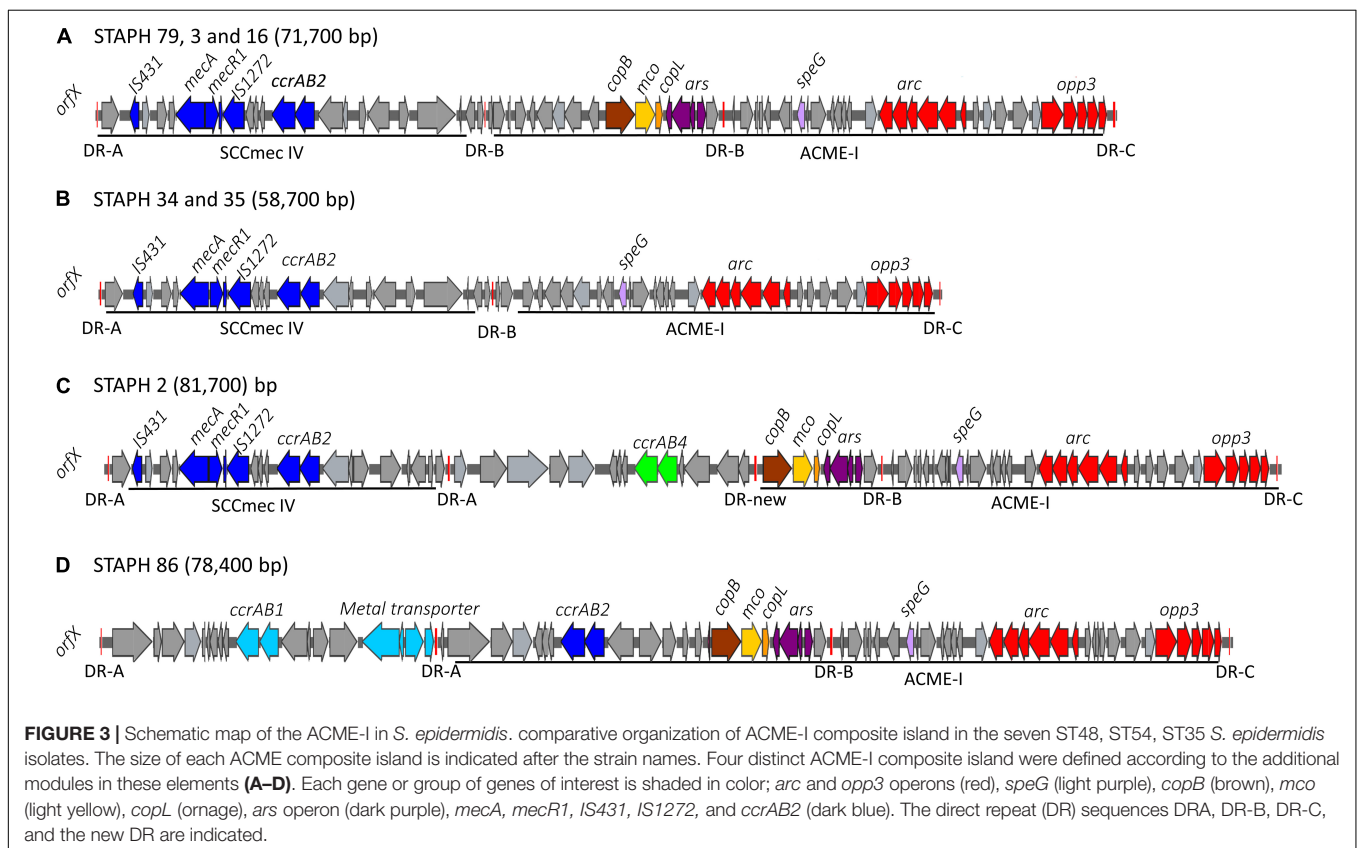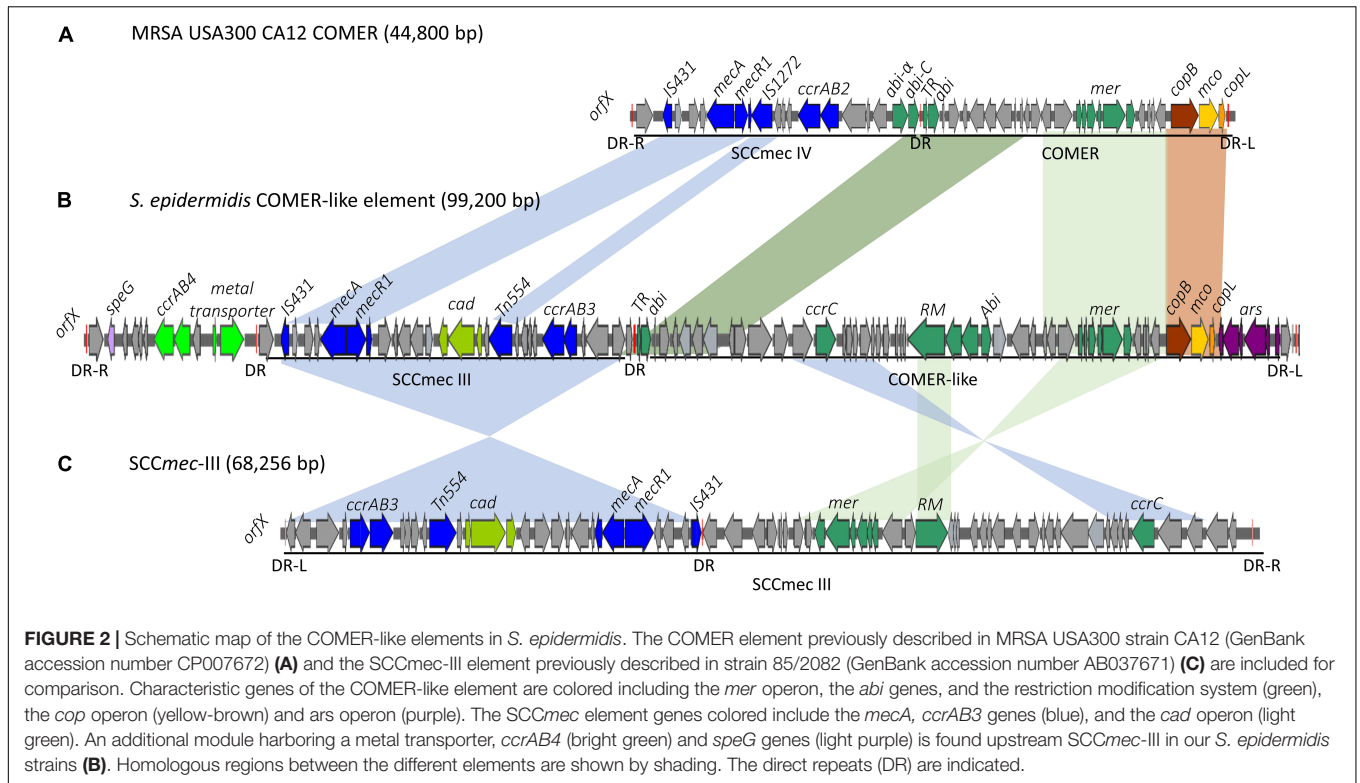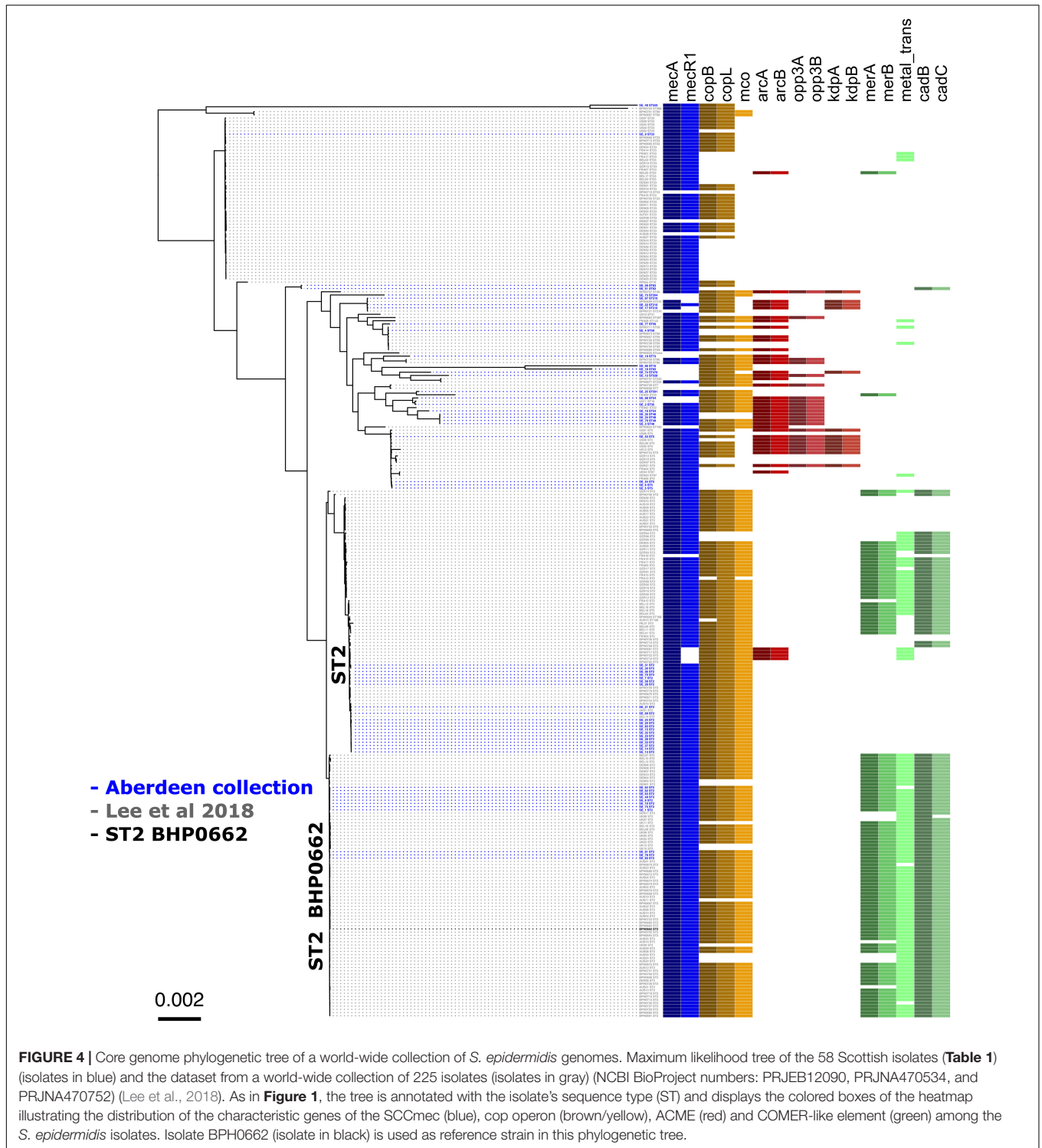
by DR_A and DR_Q was inserted between the *ars/cop* gene modules and the SCC*mec*-IV (**Figure 3C**). The ACME composite island in one ST54 isolate lacked the *mecA* gene and included only two modules located upstream the *ars/cop* genes module and the ACME-I. These two modules were flanked by DR_A, _A, and _B respectively at the 5′end in *orfX* (**Figure 3D**).

To validate the distribution of the composite SCC elements on a larger dataset and at global level, we generated a core genome phylogenetic tree that included a collection of 225 worldwide *S. epidermidis* genomes (Lee et al., 2018; **Figure 4**). The phylogenetic tree was build using the alignment of 1,898 core genes which represent 61.1% (1,706,669 bp) of the reference genome BHP662. This phylogenetic tree combining both datasets showed large clustering of ST2 isolates and their sub-lineages as found in the Scottish collection. Mapping of the key genes of our composite SCC elements, showed again exceptional stability of the COMER-like element. In the larger dataset this element mapped in all 82 isolates belonging ST2 BPH0662 sub-lineage and also partially (38/82)

to a second ST2 sub-lineage of ST2 isolates (**Figure 4**). The mapping in addition confirmed a high variability of ACME elements and their presence in multiple ST and sub-lineages. Copper resistance genes were present in most isolates, even in absence of the COMER-like and ACME elements (**Figure 4**). As expected nearly all isolates carried SCC*mec* elements.

A phenotypic analysis of metal susceptibility of these isolates was performed by disc diffusion susceptibility testing on our Scottish isolates (**Figure 5**). As no breakpoints for metal resistance exist, we determined the ECOFF (Morrissey et al., 2014). The ECOFF breakpoints, based on the normal distribution of the susceptibility, was defined using the Shapiro–Wilk test. All susceptibility data, except for copper, were not normally distributed. Still we did not define an ECOFF for iron and arsenic as the reduced inhibition zone appears to indicate intrinsic resistance of the all isolates. Isolates belonging to the ST2- BPH0662 lineage carrying the COMER-like element were found to be significantly associated with reduced susceptibility

**FIGURE 2 |** Schematic map of the COMER-like elements in *S. epidermidis*. The COMER element previously described in MRSA USA300 strain CA12 (GenBank accession number CP007672) **(A)** and the SCCmec-III element previously described in strain 85/2082 (GenBank accession number AB037671) **(C)** are included for comparison. Characteristic genes of the COMER-like element are colored including the *mer* operon, the *abi* genes, and the restriction modification system (green), the *cop* operon (yellow-brown) and ars operon (purple). The SCC*mec* element genes colored include the *mecA, ccrAB3* genes (blue), and the *cad* operon (light green). An additional module harboring a metal transporter, *ccrAB4* (bright green) and *speG* genes (light purple) is found upstream SCC*mec*-III in our *S. epidermidis* strains **(B)**. Homologous regions between the different elements are shown by shading. The direct repeats (DR) are indicated.



**FIGURE 3 |** Schematic map of the ACME-I in *S. epidermidis*. comparative organization of ACME-I composite island in the seven ST48, ST54, ST35 *S. epidermidis* isolates. The size of each ACME composite island is indicated after the strain names. Four distinct ACME-I composite island were defined according to the additional modules in these elements **(A–D)**. Each gene or group of genes of interest is shaded in color; *arc* and *opp3* operons (red), *speG* (light purple), *copB* (brown), *mco* (light yellow), *copL* (ornage), *ars* operon (dark purple), *mecA, mecR1, IS431, IS1272,* and *ccrAB2* (dark blue). The direct repeat (DR) sequences DRA, DR-B, DR-C, and the new DR are indicated.

**FIGURE 4 |** Core genome phylogenetic tree of a world-wide collection of *S. epidermidis* genomes. Maximum likelihood tree of the 58 Scottish isolates (**Table 1**) (isolates in blue) and the dataset from a world-wide collection of 225 isolates (isolates in gray) (NCBI BioProject numbers: PRJEB12090, PRJNA470534, and PRJNA470752) (Lee et al., 2018). As in **Figure 1**, the tree is annotated with the isolate's sequence type (ST) and displays the colored boxes of the heatmap illustrating the distribution of the characteristic genes of the SCCmec (blue), cop operon (brown/yellow), ACME (red) and COMER-like element (green) among the *S. epidermidis* isolates. Isolate BPH0662 (isolate in black) is used as reference strain in this phylogenetic tree.
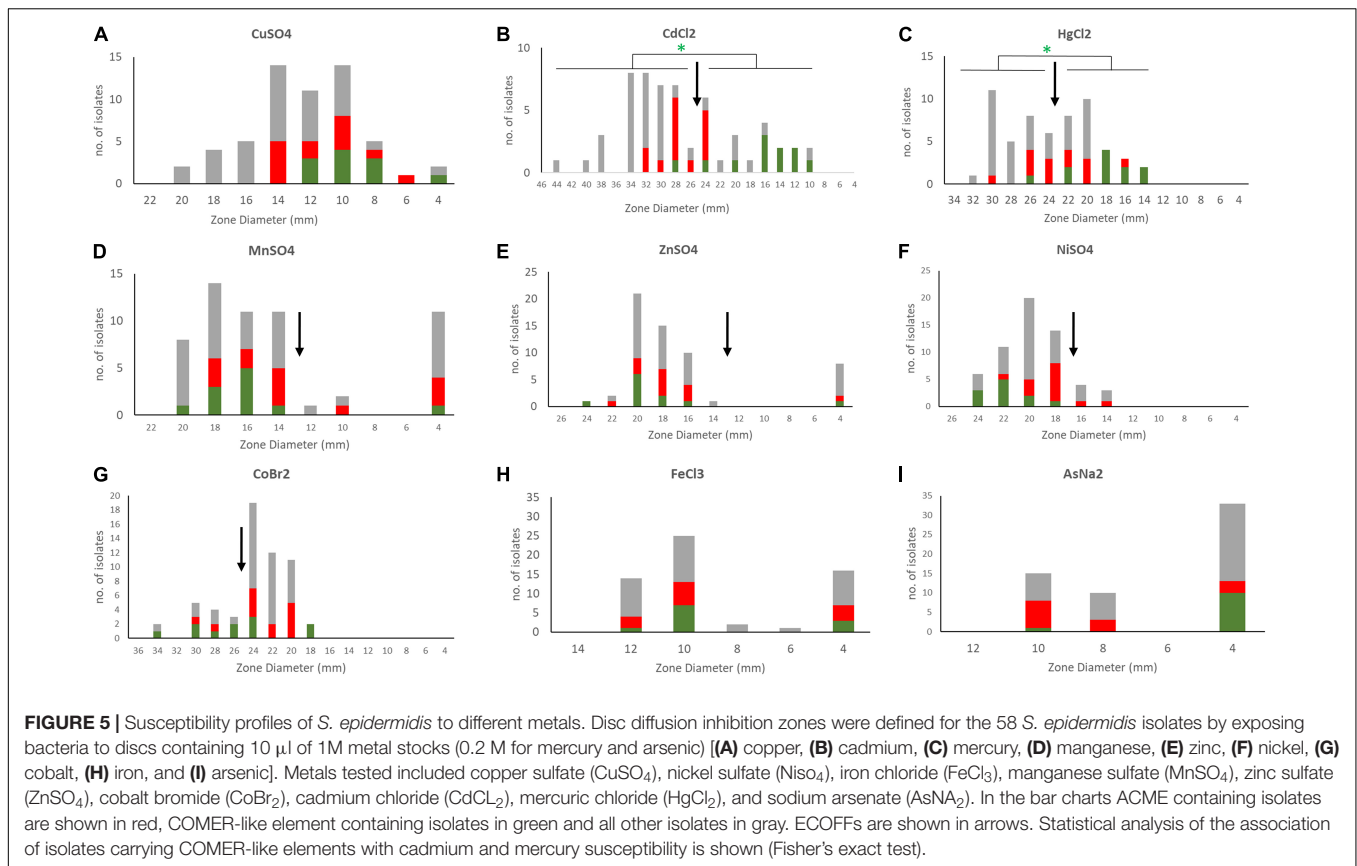
to mercury and cadmium ($p < 0.05$) using Fisher's Exact test (**Figures 5B,C**). The phenotypes match to the presence of the cadmium and mercury transporter in these strains. The linear regression model was applied to predict the disk diffusion value of the cadmium and mercury based on the presence or absence of the COMER-like element in ST2 isolates, the coefficient of

correlation for mercury was $R^2 = 0.57$ and for cadmium was $R^2 = 0.75$. No association was found for ACME-carrying isolates.

The rate of excision of the composite SCC*mec* ACME and COMER-like elements was measured by quantitative real time PCR amplification of the reconstituted chromosomal attachment/target site and the circularized elements. Results
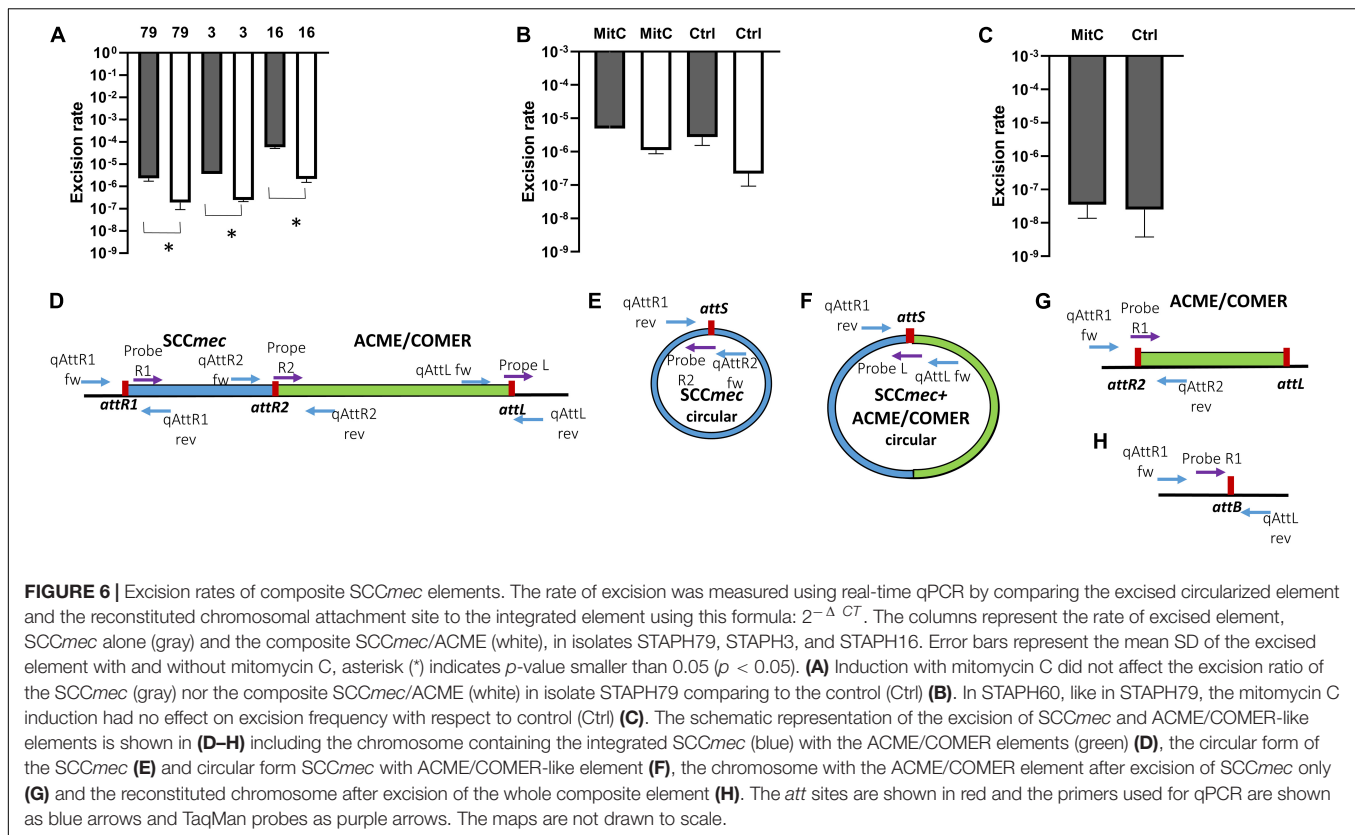
**FIGURE 5 |** Susceptibility profiles of *S. epidermidis* to different metals. Disc diffusion inhibition zones were defined for the 58 *S. epidermidis* isolates by exposing bacteria to discs containing 10 μl of 1M metal stocks (0.2 M for mercury and arsenic) [**(A)** copper, **(B)** cadmium, **(C)** mercury, **(D)** manganese, **(E)** zinc, **(F)** nickel, **(G)** cobalt, **(H)** iron, and **(I)** arsenic]. Metals tested included copper sulfate ($CuSO_4$), nickel sulfate (Niso4), iron chloride ($FeCl_3$), manganese sulfate ($MnSO_4$), zinc sulfate ($ZnSO_4$), cobalt bromide ($CoBr_2$), cadmium chloride ($CdCL_2$), mercuric chloride ($HgCl_2$), and sodium arsenate ($AsNA_2$). In the bar charts ACME containing isolates are shown in red, COMER-like element containing isolates in green and all other isolates in gray. ECOFFs are shown in arrows. Statistical analysis of the association of isolates carrying COMER-like elements with cadmium and mercury susceptibility is shown (Fisher's exact test).

were compared to the quantification of the integrated elements (considered equivalent to the total quantification of chromosomes). Results for the ACME-I isolates STAPH16, STAPH3, and STAPH79 showed that the SCC*mec*-IV element alone did excise at a frequency ranging from $5.3 \times 10^{-5}$ (isolate 16) to $2.7 \times 10^{-6}$ (isolate 79) (**Figure 6A**). The excision of the whole composite SCC*mec*-IV/ACME-I element was significantly lower ($1.7 \times 10^{-6} - 1.2 \times 10^{-7}$) ($p < 0.05$) using *t*-test (**Figure 6A**). The ratio of excision did not significantly change ($p > 0.05$) in the presence of mitomycin C for any of the isolates, as shown for isolate STAPH79 (**Figure 6B**). Results for the COMER-like element in isolate STAPH60 showed that the SCC*mec*-III excised alone at a frequency equal to $2.3 \times 10^{-8}$ and as with ACME the ratio of excision did not change with mitomycin C induction (**Figure 6C**). The whole composite SCC*mec*-III/COMER-like element excision was under the detection limit of our assay. The excision of the SCC*mec*-III is significantly lower than the SCC*mec*-IV excision by 100 times ($p < 0.05$) using *t*-test.

## DISCUSSION

In recent decades, *S. epidermidis* has emerged as a nosocomial pathogen. Genomics showed that the two *S. epidermidis* hospital-adapted lineages within ST2 are nearly pan-drug resistance (Lee et al., 2018). The evolution of *S. epidermidis* from

commensal to disease-causing bacteria is poorly investigated, although several studies suggested that *S. epidermidis* acts as a reservoir of resistance genes for *S. aureus* (Otto, 2009). Comparative genomic analysis of *S. epidermidis* clinical isolates in this study revealed a high prevalence of methicillin resistance and the MLST showed that more than half the isolates belonged to clinically predominant ST2 confirming the dissemination of this multidrug resistance lineage in our study isolates. The increased capacity of ST2 to acquire drug resistance phenotypes has been attributed to a single polymorphism in the core genome RNA polymerase gene *rpoB* (Lee et al., 2018). While this original SNP may well be at the origin of the success of ST2, the dominant presence of a large composite COMER-like element in the ST-2 BPH662 lineage is likely very significant to the success of the lineage. The COMER-like element was exceptionally stable when compared to other SCC composite structures, for example ACME (Miragaia et al., 2009; O'Connor et al., 2018b). In *S. aureus* USA300 the copper resistance phenotype conferred by the COMER element was found to be associated with increased macrophage resistance and fitness (Purves et al., 2018; Zapotoczna et al., 2018). In this study we observed only a mercury and cadmium resistance phenotype only in isolates bearing the COMER-like element, but this may be related to the wide distribution of the copper gene cluster among most *S. epidermidis* isolates. The role of the additional genes within the COMER-like element, and absent in USA300, in the success of the BPH662 lineage, cannot be inferred at this stage.

**FIGURE 6 |** Excision rates of composite SCC*mec* elements. The rate of excision was measured using real-time qPCR by comparing the excised circularized element and the reconstituted chromosomal attachment site to the integrated element using this formula: $2^{-\Delta\ CT}$. The columns represent the rate of excised element, SCC*mec* alone (gray) and the composite SCC*mec*/ACME (white), in isolates STAPH79, STAPH3, and STAPH16. Error bars represent the mean SD of the excised element with and without mitomycin C, asterisk (*) indicates *p*-value smaller than 0.05 ($p < 0.05$). **(A)** Induction with mitomycin C did not affect the excision ratio of the SCC*mec* (gray) nor the composite SCC*mec*/ACME (white) in isolate STAPH79 comparing to the control (Ctrl) **(B)**. In STAPH60, like in STAPH79, the mitomycin C induction had no effect on excision frequency with respect to control (Ctrl) **(C)**. The schematic representation of the excision of SCC*mec* and ACME/COMER-like elements is shown in **(D–H)** including the chromosome containing the integrated SCC*mec* (blue) with the ACME/COMER elements (green) **(D)**, the circular form of the SCC*mec* **(E)** and circular form SCC*mec* with ACME/COMER-like element **(F)**, the chromosome with the ACME/COMER element after excision of SCC*mec* only **(G)** and the reconstituted chromosome after excision of the whole composite element **(H)**. The *att* sites are shown in red and the primers used for qPCR are shown as blue arrows and TaqMan probes as purple arrows. The maps are not drawn to scale.

This investigation analysing the diversity of composite SCC elements identified, in addition to the well-known ACME elements characterized in *S. epidermidis,* a highly conserved COMER-like element in one of the main ST2 clusters, the BPH0662-lineage (Zamudio et al., 2019). Different types of ACME identified in this study, including ACME type IV and V, harbored the *kdp* operon linked previously to oronasal *S. epidermidis* isolates only (O'Connor et al., 2018b). The findings from oronasal *S. epidermidis* isolates harboring ACME suggested that each ACME type emerged from the respective identical or closely related ST rather than the site from which the isolates harboring ACME were recovered (O'Connor et al., 2018b). For example, isolates harboring ACME type II and V investigated in this study belonged to ST73 and ST5 respectively, the same STs harboring ACME types II and V in oronasal *S. epidermidis*. Isolates harboring ACME type I belonged to ST48 as well as ST54 and ST35 (a double locus variant of ST48) and isolates harboring ACME type IV belonged to ST210. However, one isolates with ACME type I and one isolate with ACME type IV belonged to ST528 and a new ST which is closely related to ST470 respectively, suggesting emergence from a different lineage. The variations in the ACME-composite island investigated in this study suggest the rapid evolution of ACME in *S. epidermidis*. Previous studies of ACME prevalence amongst *S. epidermidis* populations reported a higher prevalence of ACME in MSSE than MRSE (Miragaia et al., 2009; Barbier et al., 2011; Onishi et al., 2013). Our data are supportive of this finding as ACME was identified in 9/50 (18%) of the MRSE and in 4/8 (50%) of the MSSE.

In addition to confirm excision of the SCC*mec* elements as previously reported (Stojanov et al., 2015), we report circularization of the ACME element and the *S. epidermidis* COMER-like element. The excision frequency of the SCC*mec*-IV in ACME-I containing isolates 16, 3 and 79 ranged from $5.3 \times 10^{-5}$ to $2.7 \times 10^{-6}$ while the excision of the composite SCC*mec*-IV/ACME-I element was approximately 5 times lower. This finding correlates with previous studies on *S. aureus* in which the rate of excision was estimated to be lower than $10^{-4}$ (Ito et al., 1999; Stojanov et al., 2015). Interestingly, the net production of excision products in the presence of mitomycin C did not change for any of the isolates different to what observed previously by others (Liu et al., 2017). The SCC*mec*-III excision in COMER-like element containing isolate was up to 100 times lower than the SCC*mec*-IV excision. This shows a strong correlation of excision frequency and genomic variability. We hypothesize that this difference in excision of both the SCC*mec* and of the composite elements may explain the high genomic stability of the COMER-like elements compared to the high variability of the ACME elements.

## CONCLUSION

In conclusion this work identifies a large composite SCC*mec* COMER-like element in the main clinical ST-BPH662 lineage of *S. epidermidis*. The exceptional stability of this large element

supports the contribution of this element to the success of this important lineage of clinical *S. epidermidis* isolates.

## DATA AVAILABILITY STATEMENT

The datasets generated for this study can be found in the GenBank (accession numbers SAMN12840193–SAMN12840250).

## AUTHOR CONTRIBUTIONS

NA performed the bulk of the laboratory and genomic work, and wrote the manuscript. RZ provided genomic training, contributed high throughput genomic data, and participated in the writing of the manuscript. CJ and CI were involved in phenotypic of clinical isolates and DNA extraction for genome sequencing. JR was involved in genome annotation and DNA extraction. AR was co-supervisor of NA and was involved in data analysis and manuscript preparation. IG supervised the clinical isolate collection and susceptibility testing. JM was co-supervisor of NA and was involved in data analysis and manuscript preparation. KH was involved in planning of the work, data analysis, and manuscript writing. MO conceived and supervised the work and contributed to the writing of the manuscript.

## FUNDING

## ACKNOWLEDGMENTS

## REFERENCES

AltschuP, S. F., Gish, W., Miller, W., Myers, E. W., and Lipman, D. J. (1990). Basic local alignment search tool. *J. Microbiol.* 215, 403–410. doi: 10.1016/S0022-2836(05)80360-2

Aziz, R. K., Bartels, D., Best, A. A., DeJongh, M., Disz, T., Edwards, R. A., et al. (2008). The RAST server: rapid annotations using subsystems technology. *BMC Genomics* 9:75. doi: 10.1186/1471-2164-9-75

Barbier, F., Lebeaux, D., Hernandez, D., Delannoy, A.-S., Caro, V., François, P., et al. (2011). High prevalence of the arginine catabolic mobile element in carriage isolates of methicillin-resistant *Staphylococcus epidermidis*. *J. Antimicrob. Chemother.* 66, 29–36. doi: 10.1093/jac/dkq410

Berriman, M. (2003). Viewing and annotating sequence data with Artemis. *Brief. Bioinform.* 4, 124–132. doi: 10.1093/bib/4.2.124

Bolger, A. M., Lohse, M., and Usadel, B. (2014). Trimmomatic: a flexible trimmer for Illumina sequence data. *Bioinformatics* 30, 2114–2120. doi: 10.1093/bioinformatics/btu170

Darling, A. C. E. (2004). Mauve: multiple alignment of conserved genomic sequence with rearrangements. *Genome Res.* 14, 1394–1403. doi: 10.1101/gr.2289704

Diep, B. A., Gill, S. R., Chang, R. F., Phan, T. H., Chen, J. H., Davidson, M. G., et al. (2006). Complete genome sequence of USA300, an epidemic clone of community-acquired meticillin-resistant *Staphylococcus aureus*. *Lancet* 367:9.

Diep, B. A., Stone, G. G., Basuino, L., Graber, C. J., Miller, A., Etages, S., et al. (2008). The arginine catabolic mobile element and staphylococcal chromosomal cassette mec linkage: convergence of virulence and resistance in the USA300 clone of methicillin-resistant *Staphylococcus aureus*. *J. Infect. Dis.* 197, 1523–1530. doi: 10.1086/587907

Espadinha, D., Sobral, R. G., Mendes, C. I., Méric, G., Sheppard, S. K., Carriço, J. A., et al. (2019). Distinct phenotypic and genomic signatures underlie contrasting pathogenic potential of *Staphylococcus epidermidis* clonal lineages. *Front. Microbiol.* 10:1971. doi: 10.3389/fmicb.2019.01971

Gurevich, A., Saveliev, V., Vyahhi, N., and Tesler, G. (2013). QUAST: quality assessment tool for genome assemblies. *Bioinformatics* 29, 1072–1075. doi: 10.1093/bioinformatics/btt086

Hijazi, K., Mukhopadhya, I., An-Bott, F., Milne, K., Al-Jabri, Z. J., Oggioni, M. R., et al. (2016). Susceptibility to chlorhexidine amongst multidrug-resistant clinical isolates of *Staphylococcus epidermidis* from bloodstream infections. *Int. J. Antimicrob. Agents* 48, 86–90. doi: 10.1016/j.ijantimicag.2016.04.015

Ito, T., Katayama, Y., and Hiramatsu, K. (1999). Cloning and nucleotide sequence determination of the entire mec DNA of pre-methicillin-resistant *Staphylococcus aureus* N315. *Antimicrob. Agents Chemother.* 43, 1449–1458. doi: 10.1128/AAC.43.6.1449

Kaya, H., Hasman, H., Larsen, J., Stegger, M., Johannesen, T. B., Allesøe, R. L., et al. (2018). SCC *mec* finder, a web-based tool for typing of staphylococcal cassette chromosome *mec* in *Staphylococcus aureus* using whole-genome sequence data. *mSphere* 3:e00612-17. doi: 10.1128/mSphere.00612-17

Larsen, M. V., Cosentino, S., Rasmussen, S., Friis, C., Hasman, H., Marvig, R. L., et al. (2012). Multilocus sequence typing of total-genome-sequenced bacteria. *J. Clin. Microbiol.* 50, 1355–1361. doi: 10.1128/JCM.06094-11

Lee, J. Y. H., Monk, I. R., Gonçalves da Silva, A., Seemann, T., Chua, K. Y. L., Kearns, A., et al. (2018). Global spread of three multidrug-resistant lineages of *Staphylococcus epidermidis*. *Nat. Microbiol.* 3, 1175–1185. doi: 10.1038/s41564-018-0230-7

Lindgren, J. K., Thomas, V. C., Olson, M. E., Chaudhari, S. S., Nuxoll, A. S., Schaeffer, C. R., et al. (2014). Arginine deiminase in *Staphylococcus epidermidis* functions to augment biofilm maturation through pH homeostasis. *J. Bacteriol.* 196, 2277–2289. doi: 10.1128/JB.00051-14

Liu, P., Wu, Z., Xue, H., and Zhao, X. (2017). Antibiotics trigger initiation of SCCmec transfer by inducing SOS responses. *Nucleic Acids Res.* 45, 3944–3952. doi: 10.1093/nar/gkx153

Livak, K. J., and Schmittgen, T. D. (2001). Analysis of relative gene expression data using real-time quantitative PCR and the $2-\Delta\Delta CT$ method. *Methods* 25, 402–408. doi: 10.1006/meth.2001.1262

McManus, B. A., O'Connor, A. M., Kinnevey, P. M., O'Sullivan, M., Polyzois, I., and Coleman, D. C. (2017). First detailed genetic characterization of the structural organization of type III arginine catabolic mobile elements harbored by *Staphylococcus epidermidis* by using whole-genome sequencing. *Antimicrob. Agents Chemother.* 61:e01216-17. doi: 10.1128/AAC.01216-17

Méric, G., Mageiros, L., Pensar, J., Laabei, M., Yahara, K., Pascoe, B., et al. (2018). Disease-associated genotypes of the commensal skin bacterium *Staphylococcus epidermidis*. *Nat. Commun.* 9:5034. doi: 10.1038/s41467-018-07368-7

Miragaia, M., de Lencastre, H., Perdreau-Remington, F., Chambers, H. F., Higashi, J., Sullam, P. M., et al. (2009). Genetic diversity of arginine catabolic mobile element in *Staphylococcus epidermidis*. *PLoS One* 4:e7722. doi: 10.1371/journal.pone.0007722

Morrissey, I., Oggioni, M. R., Knight, D., Curiao, T., Coque, T., Kalkanci, A., et al. (2014). Evaluation of epidemiological cut-off values indicates that biocide resistant subpopulations are uncommon in natural isolates of clinically-relevant microorganisms. *PLoS One* 9:e86669. doi: 10.1371/journal.pone.0086669

Nurk, S., Bankevich, A., Antipov, D., Gurevich, A. A., Korobeynikov, A., Lapidus, A., et al. (2013). Assembling single-cell genomes and mini-metagenomes from

chimeric MDA products. *J. Comput. Biol.* 20, 714–737. doi: 10.1089/cmb.2013.0084

O'Connor, A. M., McManus, B. A., and Coleman, D. C. (2018a). First description of novel arginine catabolic mobile elements (ACMEs) types IV and V harboring a kdp operon in *Staphylococcus epidermidis* characterized by whole genome sequencing. *Infect. Genet. Evol.* 61, 60–66. doi: 10.1016/j.meegid.2018.03.012

O'Connor, A. M., McManus, B. A., Kinnevey, P. M., Brennan, G. I., Fleming, T. E., Cashin, P. J., et al. (2018b). Significant enrichment and diversity of the staphylococcal arginine catabolic mobile element ACME in *Staphylococcus epidermidis* isolates from subgingival peri-implantitis sites and periodontal pockets. *Front. Microbiol.* 9:1558. doi: 10.3389/fmicb.2018.01558

Onishi, M., Urushibara, N., Kawaguchiya, M., Ghosh, S., Shinagawa, M., Watanabe, N., et al. (2013). Prevalence and genetic diversity of arginine catabolic mobile element (ACME) in clinical isolates of coagulase-negative staphylococci: identification of ACME type I variants in *Staphylococcus epidermidis*. *Infect. Genet. Evol.* 20, 381–388. doi: 10.1016/j.meegid.2013.09.018

Otto, M. (2009). *Staphylococcus epidermidis* — the "accidental" pathogen. *Nat. Rev. Microbiol.* 7, 555–567. doi: 10.1038/nrmicro2182

Page, A. J., Cummins, C. A., Hunt, M., Wong, V. K., Reuter, S., Holden, M. T. G., et al. (2015). Roary: rapid large-scale prokaryote pan genome analysis. *Bioinformatics* 31, 3691–3693. doi: 10.1093/bioinformatics/btv421

Planet, P. J., Diaz, L., Kolokotronis, S.-O., Narechania, A., Reyes, J., Xing, G., et al. (2015). Parallel epidemics of community-associated methicillin-resistant *Staphylococcus aureus* USA300 infection in North and South America. *J. Infect. Dis.* 212, 1874–1882. doi: 10.1093/infdis/jiv320

Planet, P. J., LaRussa, S. J., Dana, A., Smith, H., Xu, A., Ryan, C., et al. (2013). Emergence of the epidemic methicillin-resistant *Staphylococcus aureus* strain USA300 coincides with horizontal transfer of the arginine catabolic mobile element and speG-mediated adaptations for survival on skin. *mBio* 4:e00889-13. doi: 10.1128/mBio.00889-13

Purves, J., Thomas, J., Riboldi, G. P., Zapotoczna, M., Tarrant, E., Andrew, P. W., et al. (2018). A horizontally gene transferred copper resistance locus confers hyper-resistance to antibacterial copper toxicity and enables survival of community acquired methicillin resistant *Staphylococcus aureus* USA300 in macrophages: *Staphylococcus aureus* copper resistance and innate immunity. *Environ. Microbiol.* 20, 1576–1589. doi: 10.1111/1462-2920.14088

Rolo, J., Worning, P., Boye Nielsen, J., Sobral, R., Bowden, R., Bouchami, O., et al. (2017). Evidence for the evolutionary steps leading to mecA-mediated β-lactam resistance in staphylococci. *PLoS Genet.* 13:e1006674. doi: 10.1371/journal.pgen.1006674

Rosario-Cruz, Z., Eletsky, A., Daigham, N. S., Al-Tameemi, H., Swapna, G. V. T., Kahn, P. C., et al. (2019). The *copBL* operon protects *Staphylococcus aureus* from

copper toxicity: CopL is an extracellular membrane–associated copper-binding protein. *J. Biol. Chem.* 294, 4027–4044. doi: 10.1074/jbc.RA118.004723

Siguier, P. (2006). ISfinder: the reference centre for bacterial insertion sequences. *Nucleic Acids Res.* 34, D32–D36. doi: 10.1093/nar/gkj014

Soroush, S., Jabalameli, F., Taherikalani, M., Amirmozafari, N., Imani Fooladi, A. A., Asadollahi, K., et al. (2016). Investigation of biofilm formation ability, antimicrobial resistance and the staphylococcal cassette chromosome mec patterns of methicillin resistant *Staphylococcus epidermidis* with different sequence types isolated from children. *Microb. Pathog.* 93, 126–130. doi: 10.1016/j.micpath.2016.01.018

Stamatakis, A. (2014). RAxML version 8: a tool for phylogenetic analysis and post-analysis of large phylogenies. *Bioinformatics* 30, 1312–1313. doi: 10.1093/bioinformatics/btu033

Stojanov, M., Moreillon, P., and Sakwinska, O. (2015). Excision of staphylococcal cassette chromosome mec in methicillin-resistant *Staphylococcus aureus* assessed by quantitative PCR. *BMC Res Notes* 8:828. doi: 10.1186/s13104-015-1815-3

Yang, Z. (1994). Maximum likelihood phylogenetic estimation from DNA sequences with variable rates over sites: approximate methods. *J. Mol. Evol.* 39, 306–314. doi: 10.1007/BF00160154

Yu, G., Smith, D. K., Zhu, H., Guan, Y., and Lam, T. T.-Y. (2017). ggtree: an r package for visualization and annotation of phylogenetic trees with their covariates and other associated data. *Methods Ecol. Evol.* 8, 28–36. doi: 10.1111/2041-210X.12628

Zamudio, R., Oggioni, M. R., Gould, I. M., and Hijazi, K. (2019). Time for biocide stewardship? *Nat. Microbiol.* 4, 732–733. doi: 10.1038/s41564-019-0360-6

Zapotoczna, M., Riboldi, G. P., Moustafa, A. M., Dickson, E., Narechania, A., Morrissey, J. A., et al. (2018). Mobile-genetic-element-encoded hypertolerance to copper protects *Staphylococcus aureus* from killing by host phagocytes. *mBio* 9:e00550-18. doi: 10.1128/mBio.00550-18